Interplay of Coulomb interaction and disorder in a two-dimensional semi-Dirac fermion system

Peng-Lu Zhao,[1] Jing-Rong Wang,[2] An-Min Wang,[1] and Guo-Zhu Liu[1,*]

[1]*Department of Modern Physics, University of Science and Technology of China, Hefei, Anhui 230026, People's Republic of China*
[2]*High Magnetic Field Laboratory, Hefei Institutes of Physical Science, Chinese Academy of Sciences,*
Hefei 230031, People's Republic of China

It was recently found that Coulomb interaction can induce a series of nontrivial spectral and transport properties in a two-dimensional semi-Dirac fermion system. Different from graphene that is basically an ordinary Fermi liquid, the Coulomb interaction in this system invalidates the Fermi liquid description over a wide range of energy scales. We present a systematic renormalization group analysis of the interplay of Coulomb interaction and quenched disorder, and show that they have substantial mutual effects on each other, which leads to a variety of quantum phase transitions and non-Fermi liquid behaviors. The low-energy behaviors of the system depend sensitively on the effective strength of Coulomb interaction and disorder.

I. INTRODUCTION

The physical effects induced by Coulomb interaction and by disorder are two important topics of theoretical condensed matter physics [1–10]. They govern most of the spectral, thermodynamic, and transport properties of quantum many body systems, and hence have been extensively studied for more than half a century [1–10].

In the normal metal possessing a finite Fermi surface, the long-range Coulomb interaction is screened by the particle-hole excitations and only leads to weak damping of the fermionic quasiparticles, which renders the validity of Landau's Fermi liquid (FL) theory [1,2]. The role of Coulomb interaction is more important in correlated electron systems that feature isolated Fermi points, such as Dirac and Weyl semimetals [8–12]. In these semimetals, the density of states (DOS) of fermion vanishes at the band touching points, so the Coulomb interaction remains long-ranged, albeit being dynamically screened [8–12]. The poorly screened Coulomb interaction may induce strong Landau damping and invalidate the ordinary FL theory. This line of thought has stimulated intense investigations in the past years, mainly in the context of graphene, a two-dimensional (2D) Dirac semimetal at zero doping. Systematic renormalization group (RG) analysis showed that Coulomb interaction does cause strong damping of Dirac fermions, but the quasiparticle residue Z_f flows to a finite constant in the low-energy regime [10,13,14]. Therefore, although the Coulomb interaction is long-ranged, the ground state of 2D Dirac fermion system is still a normal FL. The robustness of the FL description relies on the fact that the Coulomb interaction is turned into a marginally irrelevant perturbation by the substantially enhanced fermion velocity.

Recently, the effects of Coulomb interaction have been studied in a number of different kinds of semimetals. The Coulomb interaction is found to be marginally irrelevant in three-dimensional (3D) Dirac/Weyl semimetals [15–17]. RG analysis performed up to two-loop order argued that the renormalized fermion velocity may exhibit nonmonotonic energy dependence in some 3D Dirac/Weyl semimetals [17].

This is quite different from 2D Dirac semimetals, where the renormalized velocity grows monotonously as the energy is lowered. One possible reason for such a difference is that the electric charge is renormalized in 3D Dirac/Weyl semimetals, but unrenormalized in 2D Dirac semimetals [17]. After making RG analysis, Moon *et al.* showed that Coulomb interaction is relevant in 3D semimetals with quadratic band-touching points and can induce unusual non-FL behaviors [18], which confirms early studies of Abrikosov and Beneslavskii [19,20]. In 3D anisotropic Weyl semimetals, Coulomb interaction is irrelevant, as revealed in a recent RG analysis of Yang *et al.* [21] and a pioneering work of Abrikosov [22]. Theoretic studies [23,24] claimed that Coulomb interaction is marginally irrelevant in double Weyl semimetals, and gives rise to logarithmic like corrections to various observable quantities. More recently, Huh *et al.* [25] demonstrated that Coulomb interaction is also irrelevant in nodal-line semimetals.

In addition to these semimetals, a new type of 2D semimetal, often called semi-Dirac semimetal (SDSM), has also attracted considerable theoretical and experimental interest [26–49]. Close to the band touching points, the fermion dispersion is linear along one momentum direction and quadratic along the other, so a suitable name for the fermion of this system is semi-Dirac fermion (SDF). Possible materials that are predicted to realize such SDFs include deformed graphene [33–35], compressed organic conductor α-(BEDT-TTF)$_2$I$_3$ [36–38], specifically designed TiO$_2$/VO$_2$ nanostructure [39–43], and black phosphorous subject to strain [44–49]. In the noninteracting limit, the fermion DOS depends on energy ω in the form $\rho(\omega) \propto \sqrt{\omega}$ for small values of ω. The Coulomb interaction is only partially screened, and has recently been showed to induce non- or marginal FL behaviors over a wide range of energy scales [26].

Disorder effects is another important research field in condensed matter physics [3–7,9,10]. In 3D ordinary metals, the electrons become localized when the (nonmagnetic) disorder is sufficiently strong, leading to metal-insulator transition [4,5]. The scaling theory of localization leads to a striking conclusion that an arbitrarily weak disorder is able to cause weak localization of electrons in a 2D metal [4,50], provided that Coulomb interaction is ignored. Adding a weak Coulomb interaction results in analogous localization

---

*gzliu@ustc.edu.cn

195114-1

behavior in a disordered Fermi liquid [3]. It thus turns out that 2D metallic state cannot exist in zero magnetic field. Surprisingly, experiments have found compelling evidences for the existence of metallic behaviors in certain 2D dilute dirty electron systems [6], which challenges the traditional view of 2D localization. Although the microscopic mechanism of 2D metal-insulator transition is still in debate, it is universally believed that strong Coulomb interaction should play a critical role [6].

Similar to the Coulomb interaction, disorder also has different effects in various semimetals comparing to normal metals. In Dirac semimetals, backscattering is suppressed due to the chirality of massless Dirac fermions [7–10]. Strong disorder may drive the system to undergo a quantum phase transition from a ballistic state to a diffusive state by generating a finite DOS at the Fermi level and a finite scattering rate. Moreover, disorder appears in several different forms such as random energy and random fermion mass, distinguished by their coupling to fermions [7–9,51]. There are three types of most frequently studied disorders [51–56], including random chemical potential, random mass, and random gauge potential. The massless Dirac/Weyl fermions usually display distinct behaviors when they couple to different types of disorder [51–57].

When Coulomb interaction and disorder are both present, they have mutual influences on each other. Therefore, in many cases it is necessary to study their interplay [4,5]. Finkelstein [58] has developed a RG scheme to study this problem and found evidence for 2D metallic behaviors. Unfortunately, the interaction parameter flows to infinity, which invalidates the RG analysis based on the weak-coupling expansion [5,6,58]. However, if the system contains N species of fermions, it would be possible to carry out RG calculations by making series expansion in powers of $1/N$ [59], which allows one to access the strong interaction regime. In recent years, the interplay of Coulomb interaction and disorder has been studied extensively in the contexts of various semimetals [15,52–56], and found to result in quantum phase transitions, non-FL behaviors, and other unusual properties.

In this paper, we study the interplay of long-range Coulomb interaction and nonmagnetic disorder in an 2D SDF system, focusing on their mutual influences and the physical consequences produced by such an interplay. Following Isobe *et al.* [26], we will treat the Coulomb interaction between SDFs by employing a $1/N$ expansion and perform RG calculations in both the weak and strong-coupling limits, corresponding respectively to small and large values of Coulomb interaction parameter α defined below in Eq. (5). However, disorders are assumed to be weak. We consider the aforementioned three types of disorders and show that they may significantly change the role played by the Coulomb interaction. On the other hand, the role of disorder can also be substantially altered by the Coulomb interaction. The main RG results are briefly summarized in Table I, and explained in more detail in the following.

(1) In the case of random chemical potential, the effective disorder parameter C_g has an unstable fixed point $C_g^\star$. If the Coulomb interaction parameter $\alpha_N \gg 1$ and the initial value of C_g is larger than $C_g^\star$, the Coulomb interaction and random chemical potential promote each other, with α_N and

TABLE I. The main RG results are briefly summarized in the table. Col. is the abbreviation for the term Coulomb interaction, Dis. for disorder, RL for relevant, IR for irrelevant, MG for marginal, MR for marginally relevant, MIR for marginally irrelevant, and P.T. for phase transition. The parameter $\alpha_N = N\alpha$ characterizes the effective strength of Coulomb interaction, C_g is the effective strength parameter for disorder, defined by Eq. (23), with C_{g0} being its bare value, and a_c is a critical strength given by Eq. (59).

Dis. \ Col.	None ($\alpha_N = 0$)	Strong ($\alpha_N \gg 1$)	Weak ($0 < \alpha_N \ll 1$)
Chemical	MR	C_g: IR $\xrightarrow[P.T.]{C_{g0} > a_c}$ RL $\qquad$ α: IR $\xrightarrow[P.T.]{C_{g0} > a_c}$ RL	MIR
Mass	MIR	C_g: MR $\quad \alpha$: RL	
Gauge	MG	C_g: RL $\quad \alpha$: RL	

C_g growing indefinitely as the energy is lowered. This behavior most likely signals the happening of a quantum phase transition between semimetal and certain insulator. In the weak-coupling limit with $\alpha_N \ll 1$, Coulomb interaction and random chemical potential cancel each other, with α_N and C_g both flowing to the Gaussian fixed point. In different energy regimes, the system exhibits non- or marginal FL behaviors.

(2) In the case of random mass, the low-energy behaviors of the system depend sensitively on the initial values of α_N and C_g. In the strong-coupling limit $\alpha_N \gg 1$, there is a stable infrared fixed point for C_g, at which the system displays non-FL behaviors. Random mass, being marginally irrelevant in the noninteracting limit, becomes marginally relevant due to the strong Coulomb interaction. In the weak-coupling limit, there is a stable Gaussian fixed point and an unstable finite fixed point $(\alpha^\star, C_g^\star)$. Beyond $(\alpha^\star, C_g^\star)$, the parameters α_N and C_g increase at low energies. Below $(\alpha^\star, C_g^\star)$, both α_N and C_g flow to zero at low energies and the low-energy behavior is essentially governed by the Coulomb interaction.

(3) Random gauge potential and Coulomb interaction promote each other, and both α_N and C_g flow to strong-coupling regime if $\alpha_N \gg 1$. Similar to the case of random chemical potential, the SDSM might enter into certain insulating phase. In the weak-coupling limit $\alpha_N \ll 1$, there are also two fixed points for α_N and C_g: a stable Gaussian fixed point, and an unstable finite fixed point. In the latter case, the results are analogous to the other two types of disorder, and Coulomb interaction governs the system in the low-energy regime, with disorder playing an unimportant role.

Unfortunately, it is technically difficult to access the intermediate coupling regime of Coulomb interaction at present. It thus remains unclear how to reconcile the results separately obtained in the weak and strong-coupling limits. Moreover, though it seems reasonable to speculate that the ground state of the strong coupling regime is insulating, its nature is unknown and further study is required.

The rest of the paper is organized as follows. We present the whole model in Sec. II and perform detailed RG calculations in the presence of three types of disorders and Coulomb interaction in Sec. III. We ignore Coulomb interaction and analyze the impact of disorders on the low-energy behaviors of 2D SDFs in Sec. IV. In Sec. V, we solve the RG equations after taking into account the mutual influences between Coulomb interaction and disorder, and use the solutions to examine the roles played by Coulomb interaction and disorder are affected by each other. We summarize the results and briefly discuss the physical implications of our results in Sec. VI.

II. EFFECTIVE MODEL

We consider 2D SDF in the presence of both Coulomb interaction and disorder. The effective action is written in the momentum-energy space as follows:

$$S = S_f + S_b + S_g + S_{\text{dis}}, \qquad (1)$$

where

$$S_f = \sum_{i=1}^{N} \int \frac{d\omega}{2\pi} \frac{d^2k}{(2\pi)^2} \psi_i^\dagger \left(-i\omega + Ak_x^2\tau_x + vk_y\tau_y \right)\psi_i, \quad (2)$$

$$S_b = \frac{1}{2} \int \frac{d\omega}{2\pi} \frac{d^3k}{(2\pi)^2} \phi^\dagger(\omega,\mathbf{k})\left(k_x^2 + k_y^2 + k_z^2\right)\phi(\omega,\mathbf{k}), \quad (3)$$

$$S_g = \sum_{i=1}^{N} \int \frac{d\omega}{2\pi} \frac{d\omega'}{2\pi} \frac{d^2k}{(2\pi)^2} \frac{d^2k'}{(2\pi)^2} \psi_i^\dagger(\omega,\mathbf{k})$$
$$\times [ig\phi(\omega - \omega',\mathbf{k} - \mathbf{k}')]\psi_i(\omega',\mathbf{k}'). \quad (4)$$

Here, ψ_i describes a two-component spinor field with the subscript $i = 1,\ldots,N$ labeling the species of fermions. The fermions have an anisotropic dispersion, as shown by the free action term S_f, where A is the inverse of mass along the x axis and v an effective velocity along the y axis [26]. Both τ_x and τ_y are the standard Pauli matrices. The instantaneous Coulomb interaction is described by the Yukawa coupling term S_g between spinor fields ψ_i and a bosonic field ϕ that is introduced by performing a Hubbard-Stratonovich transformation [26]. The parameter g characterizes the strength of Yukawa coupling, and is given by $g = e/\sqrt{\varepsilon}$, where e is the electric charge and ε dielectric constant. It is more convenient to define a dimensionless coupling parameter α, which appears as a whole throughout all the perturbative calculations, to denote the ratio between Coulomb potential energy $E_c \sim A^{-1}vg^2$ and fermion kinetic energy $E_k \sim A^{-1}v^2$. One can easily find that

$$\alpha \equiv \frac{E_c}{E_k} = \frac{g^2}{v}. \qquad (5)$$

As explained in Ref. [26], the bosonic field ϕ is defined in 3D space, whereas the Dirac fermions are confined to the (x,y) plane. Integration over k_z gives rise to the Coulomb potential: $D_0(\mathbf{q}) \propto 1/|\mathbf{q}|$.

From the free action terms S_f and S_b, it is straightforward to obtain the free propagators of ψ and ϕ:

$$G_0(\omega,\mathbf{k}) = \frac{1}{-i\omega + Ak_x^2\tau_x + vk_y\tau_y}, \qquad (6)$$

$$D_0(\mathbf{q}) = \int \frac{dq_z}{2\pi} \frac{1}{q_x^2 + q_y^2 + q_z^2} = \frac{1}{2\sqrt{q_x^2 + q_y^2}}. \qquad (7)$$

Due to the anisotropy in the fermion dispersion, we need to perform unusual scaling transformations. In the noninteracting limit, the energy and momenta are generically rescaled as

$$\tilde{\omega} = b^z\omega \quad \tilde{k}_x = bk_x, \quad \tilde{k}_y = b^{z_1}k_y. \qquad (8)$$

The scaling dimensions are defined by $[\omega] = z$, $[k_x] = 1$, and $[k_y] = z_1$. Based on the free action term S_f, it is easy to verify that $[A] = z - 2$ and $[v] = z - z_1$. After including the corrections induced by Coulomb interaction, the parameter A and v will be renormalized and exhibit unusual dependence on varying energy scale.

The effects of Coulomb interaction on the 2D SDFs have been systematically analyzed by Isobe *et al.* in a recent work [26]. We will go one step further and include quenched disorder into the interacting SDF system. To make an unbiased analysis, we shall treat Coulomb interaction and fermion-disorder coupling on an equal footing, and study their mutual influences by means of RG approach.

The action for the fermion-disorder coupling that needs to be added to the system has the following form [7,51–55,60,61],

$$S_{\text{dis}} = \sum_{i=1}^{N} v_\Gamma \int d^2\mathbf{x}dt \, \psi_i^\dagger(\mathbf{x})\Gamma\psi_i(\mathbf{x})V(\mathbf{x}), \qquad (9)$$

where v_Γ is a coupling constant, and the function $V(\mathbf{x})$ is a quenched, random variable behaving as a Gaussian white noise, defined by

$$\langle V(\mathbf{x}) \rangle = 0, \quad \langle V(\mathbf{x})V(\mathbf{x}') \rangle = \Delta\delta^2(\mathbf{x} - \mathbf{x}'). \qquad (10)$$

Here, a dimensionless variance Δ is introduced to characterize the strength of random potential.

We will consider three different types of disorder classified by the different forms of the matrix Γ. In particular, $\Gamma = I$ for random chemical potential, $\Gamma = \tau_z$ for random mass, and $\Gamma = (\tau_x,\tau_y)$ for random gauge potential. The RG calculations are most conveniently carried out in the energy-momentum space. After making a Fourier transformation, we rewrite S_{dis} as an integration over energy and momentum in the following form:

$$S_{\text{dis}} = \sum_{i=1}^{N} \int \frac{d\omega}{2\pi} \frac{d^2\mathbf{k}}{(2\pi)^2} \frac{d^2\mathbf{k}'}{(2\pi)^2} \psi_i^\dagger(i\omega,\mathbf{k})(v_\Gamma\Gamma)\psi_i(i\omega,\mathbf{k}')$$
$$\times V(\mathbf{k} - \mathbf{k}'). \qquad (11)$$

This action will be analyzed together with Eqs. (2)–(4). In the following calculations, we choose to treat disorder using the ordinary perturbative expansion method [4,52]. Within this formalism, the coupling between fermions and random potential is represented by the diagrams presented in Figs. 2(b), 3(b), and 4.

III. FULL RG EQATIONS TO THE LEADING ORDER OF PERTURBATIVE EXPANSION

In this section, we derive the full set of RG equations for all the parameters appearing in the whole action. The calculations are carried out to the leading order of perturbative
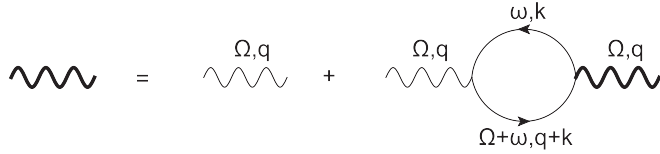
FIG. 1. One-loop Feynman diagram for dynamically screened Coulomb interaction. The solid line represents the free propagator of fermions, thin wavy line represents the bare Coulomb interaction, and thick wavy line represents the screened Coulomb interaction. The dynamical screening effects are embodied by the fermion loop to the leading order of $1/N$ expansion.

expansion. To make our analysis self-contained, we first briefly summarize the main results already obtained in Ref. [26] in Sec. III A, listing all the formulas to be used in the following calculations. The corrections induced by disorders are calculated in Sec. III B. Based on these results, we deduce all the RG equations in Sec. III C. The solutions of RG equations along with their physical implications will be presented in the next section.

A. Clean limit

To the leading order of $1/N$ expansion, the diagram for the polarization function is shown in Fig. 1, which is expressed as

$$\Pi_1(\Omega,\mathbf{q}) = -N \int \frac{d\omega}{2\pi} \frac{d^2k}{(2\pi)^2}$$
$$\times \text{Tr}[G_0(\omega,\mathbf{k})G_0(\omega+\Omega,\mathbf{k}+\mathbf{q})]. \quad (12)$$

It is hard to obtain an analytical expression for this polarization. As shown by Isobe *et al.* [26], it can be well approximated by the following *ansatz*:

$$\Pi_1(\Omega,\mathbf{q}) = -\alpha_N \Bigg[\frac{d_x A^{1/2} q_x^2}{\left(\Omega^2 + cA^2 q_x^4 + v^2 q_y^2\right)^{1/4}}$$
$$+ \frac{d_y A^{-1/2} v^2 q_y^2}{\left(\Omega^2 + cA^2 q_x^4 + v^2 q_y^2\right)^{3/4}} \Bigg], \quad (13)$$

where

$$\alpha_N \equiv N\alpha, \quad c = \left(\frac{2}{\sqrt{\pi}} \frac{\Gamma(3/4)}{\Gamma(9/4)}\right)^4,$$

$$d_x = \frac{1}{8\sqrt{\pi}} \frac{\Gamma(3/4)}{\Gamma(9/4)}, \quad d_y = \frac{1}{8\sqrt{\pi}} \frac{\Gamma(5/4)}{\Gamma(7/4)}. \quad (14)$$

After including the dynamical screening effects, as diagrammatically depicted in Fig. 1, we use Dyson equation to obtain the inverse of effective propagator of ϕ:

$$D^{-1}(\Omega,\mathbf{q}) = D_0^{-1}(\Omega,\mathbf{q}) - \Pi_1(\Omega,\mathbf{q})$$
$$= 2\sqrt{q_x^2 + q_y^2} + \alpha_N \Bigg[\frac{d_x A^{1/2} q_x^2}{\left(\Omega^2 + cA^2 q_x^4 + v^2 q_y^2\right)^{1/4}}$$
$$+ \frac{d_y A^{-1/2} v^2 q_y^2}{\left(\Omega^2 + cA^2 q_x^4 + v^2 q_y^2\right)^{3/4}} \Bigg]. \quad (15)$$

According to Fig. 2(a), the fermion self-energy correction due to the Coulomb interaction can be computed as
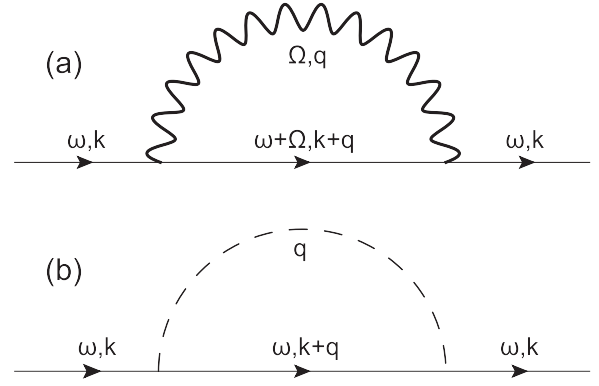

FIG. 2. Leading order corrections to the fermion self-energy due to (a) Coulomb interaction; (b) disorder. In diagram (b), the dashed line stands for disorder, corresponding to the mean value $\langle V(\mathbf{x})V(\mathbf{x}')\rangle$, and the coupling between fermion and disorder is represented by the intersection of solid and dashed lines.

follows:

$$\Sigma_1(i\omega,\mathbf{k}) = -g^2 \int \frac{d\Omega d^2q}{(2\pi)^3} G_0(\omega+\Omega,\mathbf{k}+\mathbf{q})D(\Omega,\mathbf{q})$$
$$= \Sigma_\omega i\omega - \Sigma_{k_x} A k_x^2 \tau_x - \Sigma_{k_y} v k_y \tau_y, \quad (16)$$

where

$$\Sigma_\omega = \gamma_z l, \quad \Sigma_{k_x} = \Sigma_\omega + \gamma_A l, \quad \Sigma_{k_y} = \Sigma_\omega + \gamma_v l. \quad (17)$$

Here, a varying length scale $l = \log(\Lambda/\mu)$ is defined and will be used later.

To compute $\Sigma_1(i\omega,\mathbf{k})$, we need to substitute Eq. (15) into Eq. (16). However, $D(\Omega,\mathbf{q})$ is formally very complicated, so it is hard to get an analytic expression for $\Sigma_1(i\omega,\mathbf{k})$. As demonstrated in Ref. [26], it is convenient to consider two limits $\alpha_N \gg 1$ and $\alpha_N \ll 1$ separately. In a given Dirac fermions system, the fermion flavor is fixed at certain value, but the parameter α can be tuned by changing the surrounding environment or other variables. Therefore, these two limits can be achieved by tuning α to take a large or small value, corresponding to strong or weak-coupling limit, respectively. In the strong-coupling limit with $\alpha_N \gg 1$, $\Pi_1(\Omega,\mathbf{q})$ is much more important than $D_0^{-1}(\Omega,\mathbf{q})$. Conversely, $D_0^{-1}(\Omega,\mathbf{q})$ is much more important than $\Pi_1(\Omega,\mathbf{q})$ in the weak-coupling limit with $\alpha_N \ll 1$. In both cases, $D^{-1}(\Omega,\mathbf{q})$ is simple enough to lead to an analytical expression for $\Sigma_1(i\omega,\mathbf{k})$. It was found in Ref. [26] that the anomalous exponents defined in Eq. (16) are

$$\gamma_z = \frac{\sqrt{15}\log(\alpha_N)}{\pi^{(3/2)}N}, \quad \gamma_A = \frac{0.1261}{N}, \quad \gamma_v = \frac{0.3625}{N} \quad (18)$$

in the strong-coupling limit, and

$$\gamma_z = \frac{3\alpha_N}{8\pi^2 N}, \quad \gamma_A = \frac{\alpha_N |\ln \alpha_N|}{2\pi^2 N}, \quad \gamma_v = \frac{\alpha_N}{4\pi^2 N} \quad (19)$$

in the weak-coupling limit.

All the vertex corrections for Coulomb interaction are shown in Fig. 3. As demonstrated in Ref. [26], at vanishing
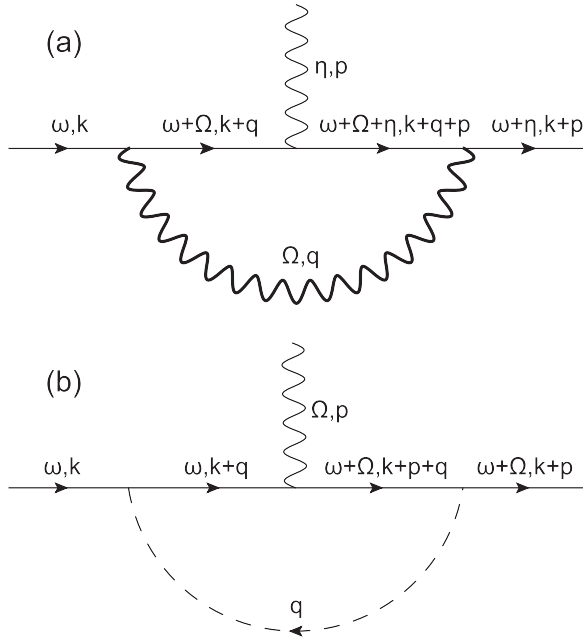
FIG. 3. One-loop Coulomb vertex correction due to (a) Coulomb interaction, (b) disorder.

external momenta and energy, the vertex correction due to Coulomb correction shown in Fig. 3(a) is [26]

$$\delta g_1 = -ig^3 \int \frac{d\Omega d^2 q}{(2\pi)^3} G_0(\Omega, \mathbf{q}) G_0(\Omega, \mathbf{q}) D(\Omega, \mathbf{q})$$
$$\equiv (ig)\Sigma_\omega. \tag{20}$$

B. Corrections with Fermion-disorder interaction

The leading correction to the fermion self-energy due to fermion-disorder interaction is shown in Fig. 2(b), which is computed as follows:

$$\Sigma_{\text{dis}}(i\omega) = \Delta v_\Gamma^2 \int \frac{d^2 \mathbf{q}}{(2\pi)^2} \Gamma G_0(i\omega, \mathbf{q}) \Gamma$$
$$= i\omega \frac{\Delta v_\Gamma^2}{2\pi v^2} \frac{1}{\bar{A}} l + \frac{\Delta v_\Gamma^2}{2\pi v} \Lambda \Gamma \tau_x \Gamma, \tag{21}$$

where $\bar{A} \equiv \frac{A\Lambda}{v}$. Similar to the case studied in Ref. [26], the self-energy contains a constant contribution $\Sigma_{\text{dis}}(0,0) = \frac{\Delta v_\Gamma^2}{2\pi v} \Lambda \Gamma \tau_x \Gamma$, which is not divergent in the infrared region and thus can be safely neglected. Moreover, Σ_{dis} does not depend on momenta since the quenched disorders are static. It is also independent of the specific sort of the disorder. To capture these two important features, we rewrite the self-energy as

$$\Sigma_{\text{dis}} = i\omega C_g l, \tag{22}$$

where a dimensionless parameter is defined to characterize the effective strength of disorder:

$$C_g \equiv \frac{\Delta v_\Gamma^2}{2\pi v^2} \frac{1}{\bar{A}}. \tag{23}$$

We next consider the corrections to the fermion-disorder vertex, which receive contributions from both Coulomb
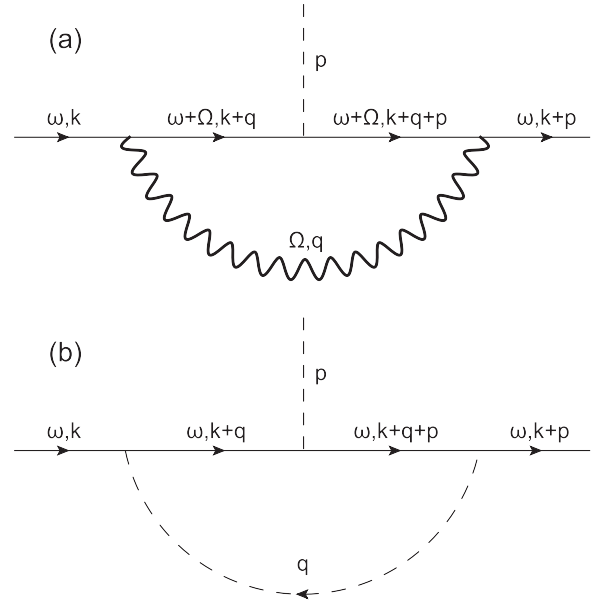

FIG. 4. One-loop fermion-disorder vertex correction due to (a) Coulomb interaction, (b) disorder.

interaction and fermion-disorder interaction, represented by the diagrams shown in Fig. 4. At zero external momenta, the vertex correction due to disorder, corresponding to Fig. 4(b), is

$$V_{\text{dis}} = \Delta v_\Gamma^2 \int \frac{d^2 \mathbf{q}}{(2\pi)^2} \Gamma G_0(i\omega, \mathbf{q}) v_\Gamma \Gamma G_0(i\omega, \mathbf{q}) \Gamma, \tag{24}$$

which yields

$$V_{\text{dis}} = C_D (v_\Gamma \Gamma) l, \tag{25}$$

where $C_D = C_g$ for random chemical potential, $C_D = 0$ for both of the two components of random gauge potential, and $C_D = -C_g$ for random mass.

According to Fig. 4(a), at zero external momenta and energy, the disorder vertex correction due to Coulomb interaction is given by

$$V_c = -g^2 \int \frac{d\Omega d^2 \mathbf{q}}{(2\pi)^3} G_0(\Omega, \mathbf{q})(v_\Gamma \Gamma) G_0(\Omega, \mathbf{q}) D(\Omega, \mathbf{q}), \tag{26}$$

Here, we borrow some definitions from Ref. [26] and then obtain

$$V_c = (v_\Gamma \Gamma)(\Sigma_\omega + \gamma_D l). \tag{27}$$

In the strong-coupling limit, $\gamma_D = 0$ for random chemical potential, $\gamma_D = 1.1564/N$ for random mass, $\gamma_D = 0.7939/N$ and $\gamma_D = 0.3625/N$ for the $\Gamma = \tau_x$- and $\Gamma = \tau_y$ component of random gauge potential, respectively. In the weak-coupling limit, $\gamma_D = 0$ for random chemical potential, $\gamma_D = 13\alpha_N/4\pi^2 N$ for random mass, $\gamma_D = 3\alpha_N/\pi^2 N$ for the τ_x component and $\gamma_D = \alpha_N/4\pi^2 N$ for the τ_y component of random gauge potential.

Moreover, disorder will produce another correction to Coulomb interaction vertex, as shown in Fig. 3(b). This correction will be calculated here to illustrate that g is actually not renormalized within the framework of Wilsonian RG

scheme. According to Fig. 3(b), it is easy to get

$$\delta g_2 = \Delta v_\Gamma^2 \int \frac{d^2\mathbf{q}}{(2\pi)^2} \Gamma G_0(\mathbf{q})(ig)G_0(\mathbf{q})\Gamma$$
$$= (ig)C_g l. \tag{28}$$

C. Derivation of RG equations

To perform RG analysis, it is convenient to define

$$\tilde{\psi} = \sqrt{Z_\psi}\psi, \quad \tilde{\phi} = \sqrt{Z_\phi}\phi, \quad \tilde{A} = Z_A A,$$
$$\tilde{v} = Z_v v, \quad \tilde{g} = Z_g g, \quad \tilde{v}_\Gamma = Z_\Gamma v_\Gamma. \tag{29}$$

Before applying rescaling transformation to the effective action, we need to first determine how the random potential transforms under the scaling given by Eq. (8). In the spirit of RG theory [62], to specify how a field operator transforms, the standard method is to require that its kinetic term remains invariant. However, the random potential $V(\mathbf{x})$ does not have its own kinetic term. To proceed, we write the Gaussian white-noise distribution in the momentum space as

$$\langle V(\mathbf{k}_1)V(\mathbf{k}_2)\rangle = \Delta \int \frac{d^2\mathbf{x}}{(2\pi)^2} e^{i(\mathbf{k}_1+\mathbf{k}_2)\cdot\mathbf{x}}$$
$$= \Delta b^{z_1+1} \int \frac{d^2\tilde{\mathbf{x}}}{(2\pi)^2} e^{i(\tilde{\mathbf{k}}_1+\tilde{\mathbf{k}}_2)\cdot\tilde{\mathbf{x}}}. \tag{30}$$

By requiring the disorder distribution Eq. (30) to be invariant under scaling transformations, we find that

$$\tilde{V}(\tilde{\mathbf{k}}) = V(\mathbf{k})b^{\frac{-1-z_1}{2}}, \tag{31}$$

which will be used to carry out RG scaling transformations.

Based on the above results, we eventually obtain the following complete set of flow equations:

$$\frac{d\ln A}{dl} = \gamma_A - C_g + z - 2, \tag{32}$$

$$\frac{d\ln v}{dl} = \gamma_v - C_g + z - z_1, \tag{33}$$

$$\frac{d\ln g}{dl} = \frac{z - z_1}{2}, \tag{34}$$

$$\frac{d\ln v_\Gamma}{dl} = \gamma_D + C_D - C_g + z - \frac{1+z_1}{2}. \tag{35}$$

As explained in Ref. [26], the full vertex of Coulomb interaction is given by the product gZ_f, which is guaranteed by charge conservation to be unrenormalized. This property is reflected in Eq. (34), in which we use g to represent the product gZ_f for notational simplicity.

In the above RG equations, the flowing parameter all have a finite scaling dimension. To make a scaling-independent analysis of the effects of Coulomb interaction and disorder, we need to derive flow equations of dimensionless parameters. Using Eqs. (33) and (34), we obtain the flow equation for the Coulomb interaction parameter

$$\frac{d\ln \alpha_N}{dl} = C_g - \gamma_v, \tag{36}$$

where α_N is defined by the unrenormalized vertex g. For fermion-disorder coupling parameter C_g, the corresponding

flow equation is

$$\frac{d\ln C_g}{dl} = 2\gamma_D - \gamma_A - \gamma_v + 2C_D. \tag{37}$$

We now have already obtained the RG equations for all the model parameters. It is important to stress that the parameters γ_z, γ_A, γ_v, and γ_D take different values in the strong and weak-coupling limits, which will be explained whenever necessary below.

By setting $C_g = 0$ and $z = z_1 = 2$, Eqs. (32), (33), and (36) recover the RG equations for A, v, and α previously obtained in Ref. [26] in the clean limit. Isobe *et al.* [26] have studied the effects of Coulomb interaction on various observable quantities by performing a RG analysis, and revealed that over a wide range of energies the Coulomb interaction is a relevant perturbation in the strong-coupling limit. In particular, Coulomb interaction generates two anomalous exponents γ_A and γ_v for parameters A and v, respectively. One can verify that $A(l)$ and $v(l)$ increase exponentially with growing l, whereas the quasiparticle residue $Z_f(l)$ decrease exponentially with growing l. In the weak-coupling limit, Coulomb interaction becomes less important in the low-energy regime and does not generate any anomalous dimension for A and v. In this case, $A(l)$ exhibits a complicated dependence on length scale l, and $v(l)$ grows as certain powers of l. However, the residue $Z_f(l)$ decreases as certain powers of l, thus the system displays marginal FL behavior at low energies [26].

The aim of this work is to analyze the roles played by Coulomb interaction and disorders based on the RG equations derived in both the strong and weak-coupling limits. Before studying the interplay of Coulomb interaction and disorder, it is helpful to first drop Coulomb interaction and only consider the fermion-disorder coupling, which will be addressed in next section.

IV. DISORDER EFFECTS IN THE ABSENCE OF COULOMB INTERACTION

In this section, we consider the influence of three types of disorder on the low-energy properties of 2D SDFs by simply ignoring the Coulomb interaction. We first make a detailed analysis of the possible RG solutions by setting $\alpha = 0$, then discuss the low-energy behaviors of renormalized parameters A and v, and finally compute the quasiparticle residue Z_f to determine whether disorders lead to non-FL behaviors of the system.

A. Solutions of RG equations

In the noninteracting limit, the RG equations become

$$\frac{d\ln A}{dl} = -C_g + z - 2, \tag{38}$$

$$\frac{d\ln v}{dl} = -C_g + z - z_1, \tag{39}$$

$$\frac{d\ln C_g}{dl} = 2C_D. \tag{40}$$

Notice that the flow equation of C_g is independent of the other two equations, so it is possible to first obtain the solution of C_g and analyze its l dependence.

In the case of random chemical potential, we have

$$\frac{dC_g}{dl} = 2C_g^2, \tag{41}$$

which has the following solution:

$$C_g(l) = \frac{C_{g0}}{1 - 2C_{g0}l}. \tag{42}$$

Here, C_{g0} is the value of parameter $C_g(l)$ defined at the upper energy limit Λ. There exists a characteristic length scale $l_c = 1/2C_{g0}$. Below l_c, $C_g(l)$ is an increasing function of l, thus random chemical potential is a marginal relevant perturbation in the low-energy regime. As l approaches l_c from below, C_g appears to be divergent. We need to understand such a superficial divergence with caution. The perturbative RG calculations are reliable only for small values of C_g, so we cannot expect to have a really divergent C_g. Instead, the unbounded increase of C_g with growing l below l_c is most likely a signature that random chemical potential causes an instability of the system and turns the semimetallic state into a disorder controlled diffusive state [15,63–68].

For random mass, the equation for C_g is

$$\frac{dC_g}{dl} = -2C_g^2. \tag{43}$$

Its solution is

$$C_g(l) = \frac{C_{g0}}{1 + 2C_{g0}l}. \tag{44}$$

It is easy to verify that $C_g(l) \to 0$ as $l \to +\infty$, which implies that random mass is a marginally irrelevant perturbation to the system.

For random gauge potential, we find

$$\frac{dC_g}{dl} = 0 \Rightarrow C_g(l) = C_{g0}. \tag{45}$$

It therefore turns out that random gauge potential is marginal and C_g is a l-independent constant.

We next use the flowing behavior of C_g to analyze the impact of disorders on the low-energy physical properties of 2D SDFs. According to Ref. [21], the scaling parameters z and z_1 can be fixed at $z_1 = z = 2$, thus both A and v are taken to be marginal parameters at the starting point. We learn from Eqs. (38) and (39) that A and v might be substantially modified by disorders due to the existence of C_g.

In the case of random chemical potential, A and v depend on l as

$$\frac{A(l)}{A_0} = \frac{v(l)}{v_0} = \sqrt{1 - 2C_{g0}l}. \tag{46}$$

As l grows approaching l_c, both $A(l)$ and $v(l)$ vanish. For random mass, we use Eq. (44) to obtain

$$\frac{A(l)}{A_0} = \frac{v(l)}{v_0} = \frac{1}{\sqrt{1 + 2C_{g0}l}}, \tag{47}$$

which shows that $A(l)$ and $v(l)$ vanish in the limit $l \to +\infty$. For random gauge potential, one can similarly show that $A(l)$ and $v(l)$ decrease exponentially with growing l and rapidly

flow to zero as $l \to +\infty$. Therefore, we conclude that all the three types of disorders can drive A and v to vanish in the lowest energy limit. Apparently, disorders have completely different influences on A and v from Coulomb interaction, which tends to increase A and v in the low-energy regime.

B. Quasiparticle residue Z_f

In any interacting fermion system, the quasiparticle residue Z_f serves as a crucial quantity to judge whether a correlated many fermion system can be well described by normal FL theory: Z_f is finite in a normal FL, but vanishes in a marginal FL and a non-FL. This quantity is usually defined by the wave renormalization functions follows:

$$Z_f = \frac{1}{1 - \frac{\partial \mathrm{Re}\Sigma^R(\omega)}{\partial \omega}}, \tag{48}$$

where $\mathrm{Re}\Sigma^R(\omega)$ is the real part of retarded fermion self-energy function. Taking advantage of the RG results, it is more convenient to write it in the form [55]

$$Z_f = e^{-\int_0^l C_g dl}, \tag{49}$$

which explicitly includes the impact of disorder through the parameter C_g. Making derivative with respect to l, we find that

$$\frac{d\ln Z_f}{dl} = -C_g. \tag{50}$$

Therefore the l dependence of $Z_f(l)$ is indeed the same as that of $A(l)$ and $v(l)$. For convenience, here we list the results as follows:

$$Z_f(l) = \begin{cases} \sqrt{1 - 2C_{g0}l} & \text{(random chemical potential)} \\ 1/\sqrt{1 + 2C_{g0}l} & \text{(random mass)} \\ e^{-C_{g0}l} & \text{(random gauge potential)} \end{cases}. \tag{51}$$

For random chemical potential, Z_f vanishes when l approaches l_c from below. Recall that the fermion velocities also decrease rapidly to zero at the same finite energy scale. These unusual behaviors indicate the instability of Fermi liquid and may, as aforementioned, signal the transition into a diffusive state.

For the other two types of disorders, $Z_f \to 0$ as $l \to \infty$, indicating the breakdown of ordinary FL description. However, there is a subtle difference in the quantitative l-dependence of Z_f between random mass and random gauge potential. To illustrate this difference, we now compute the fermion damping rate. For random mass, the corresponding Z_f can be approximated by

$$Z_f(l) \propto \frac{1}{l} \tag{52}$$

for sufficiently large l. Using Eq. (48) and the scaling relation $\omega = \omega_0 e^{-2l}$, where ω_0 is the upper limit of fermion energy, we obtain

$$\mathrm{Re}\Sigma^R(\omega) \propto \omega \ln\left(\frac{\omega_0}{\omega}\right). \tag{53}$$

Based on the Kramers-Kronig (KK) relation, we can compute the imaginary part of retarded fermion self-energy and get

$$\text{Im}\Sigma^R(\omega) \propto \omega, \tag{54}$$

which is linear in ω and thus signals the appearance of marginal FL behavior. For random gauge potential, we find that

$$\text{Re}\Sigma^R(\omega) \propto \omega^{1-\delta/2}, \tag{55}$$

where $\delta = C_{g0}$. Applying the KK relation leads us to

$$\text{Im}\Sigma^R(\omega) \propto \omega^{1-\delta/2}, \tag{56}$$

which implies that the system displays non-FL behavior since $C_{g0} > 0$. We thus conclude that, random mass leads to marginal FL behavior, whereas random gauge potential produces non-FL behavior. As a comparison, random gauge potential [7] also induces non-FL behavior of massless nodal fermions in d-wave superconductors [69].

V. INTERPLAY OF COULOMB INTERACTION AND DISORDER

In this section, we include both Coulomb interaction and disorder, and investigate their mutual influence as well as the possible phase transitions driven by their interplay. The consideration is based on the full set of RG equations obtained in the strong and weak coupling limits respectively. Following the procedure of Sec. IV, we will determine the l dependence of C_g, specify the (ir)relevance of disorders, examine the low-energy behaviors of A and v, and finally study the physical effects of Coulomb interaction.

A. Random chemical potential

In this section, we present a detailed RG analysis in the case of random chemical potential. The bare value of α is strongly material dependent. For instance, $\alpha \approx 0.41$ in VO$_2$ [39,41,70] and $\alpha \approx 0.44$ in black phosphorus [49,71]. The value of α could be greatly amplified when the system is delicately tuned to certain quantum critical point. Once α exceeds unity, i.e., $\alpha > 1$, the ordinary perturbation expansion breaks down. However, since we perform RG analysis by utilizing $1/N$ expansion, in principle, α can take a large value, and so does α_N. As demonstrated in Ref. [26], the RG analysis is greatly simplified in the large and small α_N limits, but the intermediate coupling regime is technically hard to handle. In the following, we will consider the strong and weak-coupling limits separately. The same procedure can be directly applied to study the cases of random mass and random gauge potential, which are presented in the rest two subsections.

1. Strong-coupling limit

In the strong-coupling limit, the flow equation of C_g can be written as

$$\frac{dC_g}{dl} = (2C_g - \gamma_A - \gamma_v)C_g, \tag{57}$$

which has the following solution:

$$C_g(l) = \frac{a_c C_{g0}}{C_{g0} - (C_{g0} - a_c)e^{2a_cl}}, \tag{58}$$

where

$$a_c = \frac{\gamma_A + \gamma_v}{2} = \frac{0.2443}{N}. \tag{59}$$

We have already illustrated in the last section that the parameter C_g for random chemical potential increases monotonously with growing l in the noninteracting limit with $\alpha_N = 0$. After including the Coulomb interaction, there appears a critical value $C_g^\star = a_c$. When $C_{g0} < a_c$, the parameter C_g flows to zero in the long wavelength (low-energy) limit $l \rightarrow \infty$, hence weak random chemical potential is a irrelevant perturbation. Conversely, if $C_{g0} > a_c$, the renormalized parameter C_g increases rapidly with growing l and formally flows to infinity at a finite length scale $l_c' = 1/2a_c \ln[C_{g0}/(C_{g0} - a_c)]$. It thus turns out that there are two infrared fixed points: $C_g^\star = 0$, defining a stable Gaussian fixed point; $C_g^\star = a_c$, corresponding to an unstable fixed point. The schematic flowing behavior of C_g is presented in Figs. 5(a) and 5(b). As explained in the last section, the most reasonable interpretation of the unbounded increase of C_g is that the system undergoes a quantum phase transition, with the unstable fixed point $C_g^\star = a_c$ being the quantum critical point. The Gaussian fixed point of C_g does not exist in the noninteracting limit, and is induced by the addition of strong Coulomb interaction.

After identifying the fixed points of C_g, we turn to consider the impact of random chemical potential on the fate of Coulomb interaction strength α_N. In a clean 2D SDF system, we know from Ref. [26] that α_N decreases monotonously as the energy scale is lowered. In the presence of weak random chemical potential with $C_{g0} < a_c$, we infer from Eq. (36) that $\alpha_N \rightarrow 0$ in the lowest-energy limit. In this case, random chemical potential is too weak to induce any sizable change of the role played by the Coulomb interaction. In contrast, when $C_{g0} > a_c$, α_N increases with growing l and formally diverges as $l \rightarrow l_c'$. An apparent indication of this result is that the importance of Coulomb interaction is significantly enhanced by strong random chemical potential.

The superficial divergence of α_N and C_g needs to be properly understood. In the noninteracting limit with $\alpha_N = 0$, the unbounded increase of disorder parameter C_g in the low-energy regime could be interpreted as a quantum phase transition of the system into a disorder-dominant diffusive state [15,63–68]. However, if both C_g and α_N flow to very large values, the system may exhibit other kinds of states. For instance, the system might be turned into an excitonic insulator [52,54]. Another possibility is the formation of Wigner lattice, which is known to be the ground state of 2D electron gas when the Coulomb interaction is sufficiently strong [72]. The nature of the ground state of the system at large values α_N and C_g is currently unclear and needs to be further studied.

In the following, we focus on the low-energy properties of the system at the Gaussian fixed point. Although α_N and C_g both flow to zero in the low-energy regime at the Gaussian fixed point, their physical effects on the system cannot be simply neglected. Before eventually flowing to zero, Coulomb interaction and random chemical potential lead to considerable corrections to the quantities A and v.

In the clean limit, both A and v increase as the energy is lowered due to the Coulomb interaction. If the noninteracting SDFs couple to random chemical potential, A and v are driven
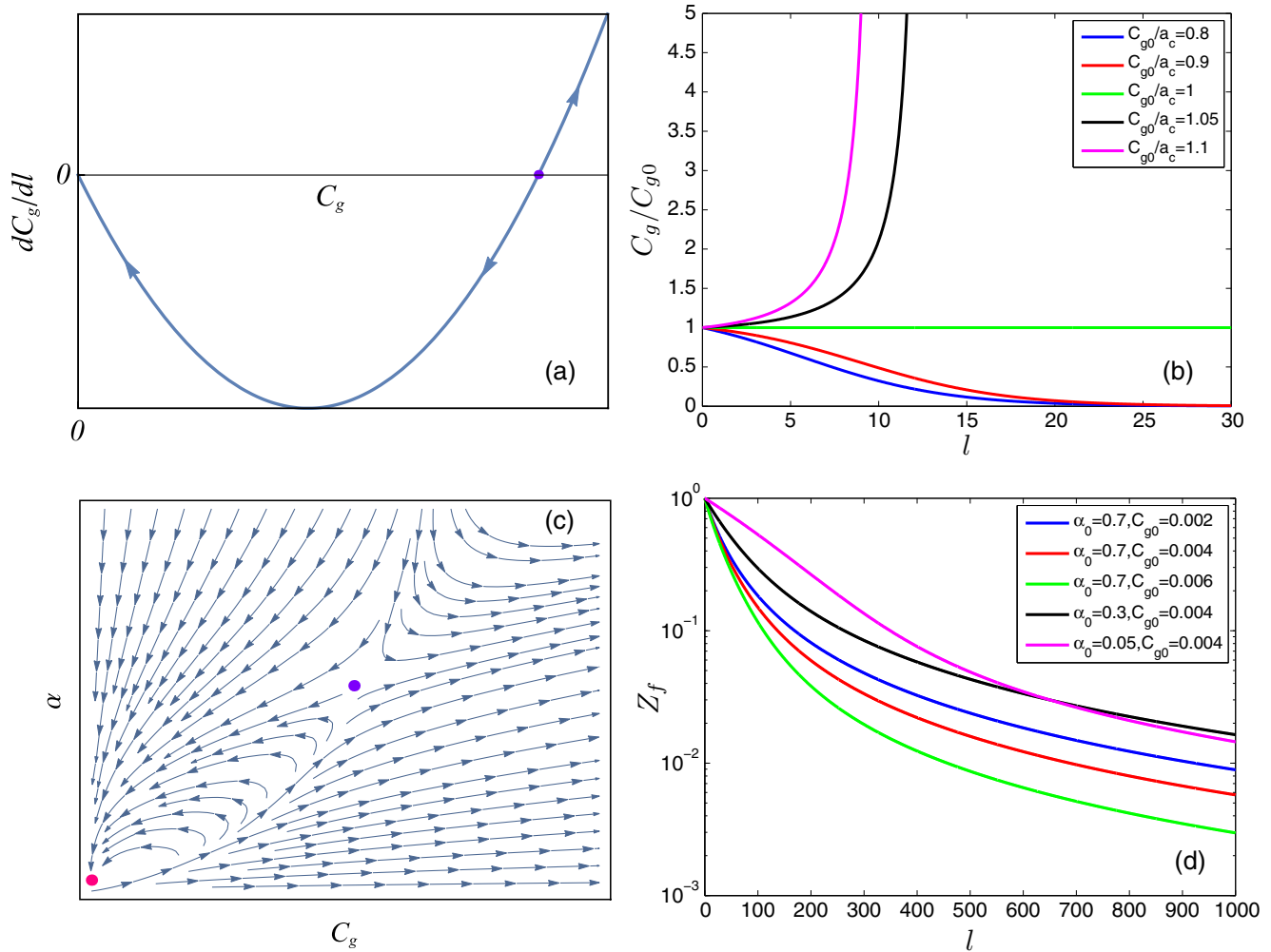
FIG. 5. (a) Flow diagram of C_g in the case of random chemical potential. There is a stable Gaussian fixed point $C_g = 0$ and a finite unstable fixed point $C_g = a_c$. (b) Dependence of C_g on the running scale for different initial values. (c) Flow diagram in the parameter space spanned by α and C_g, with α being in the weak-coupling limit. Red point denotes the stable Gaussian fixed point, and purple point represents the unstable fixed point. (d) Flow of Z_f obtained in the weak coupling limit. Here, the fermion flavor is assumed to be $N = 2$.

to vanish at low energies. Apparently, Coulomb interaction and random chemical potential give rise to distinct low-energy behaviors of A and v. In the presence of both Coulomb interaction and random chemical potential, we substitute Eq. (58) into Eq. (32) and Eq. (33) with chosen values $z_1 = z = 2$, and then obtain

$$F(l) = F_0 e^{(\gamma_F - a_c)l} \sqrt{t_c - (t_c - 1)e^{2a_c l}}, \qquad (60)$$

where $t_c \equiv C_{g0}/a_c$ and a function F is introduced to represent A or v. As C_g increases from the unstable fixed point, where $t_c > 1$, both A and v tend to vanish at a finite length scale $l = l_c'$. However, as C_g flows to its Gaussian fixed point, the function $F(l)$ exhibits the following asymptotic behavior:

$$F(l)\big|_{l \to \infty} \sim F_0 e^{(\gamma_F - a_c)l}\big|_{l \to \infty}. \qquad (61)$$

Since $\gamma_A < a_c < \gamma_v$, we find that A still flow to zero, but v grows indefinitely in the lowest energy limit. Comparing to the clean case, the anomalous exponent γ_A induced by Coulomb interaction is eliminated by random chemical potential, whereas the anomalous exponent γ_v is reduced.

The above results ought to be further examined. As C_g approaches the Gaussian fixed point, α_N flows to zero at very low energies. However, this conclusion is obtained based on the assumption that Coulomb interaction is in the strong-coupling limit. It is necessary to directly consider the case of weak Coulomb interaction and verify whether the above results are reliable. This will be presented in the next subsection.

2. Weak-coupling limit

We now consider the case of weak-coupling limit with $\alpha_N \ll 1$. In the case of random chemical potential, we obtain the flow equations:

$$\frac{d \ln \alpha_N}{dl} = C_g - \frac{\alpha_N}{4\pi^2 N}, \qquad (62)$$

$$\frac{d \ln C_g}{dl} = 2C_g - \frac{\alpha_N |\ln \alpha_N|}{2\pi^2 N} - \frac{\alpha_N}{4\pi^2 N}. \qquad (63)$$

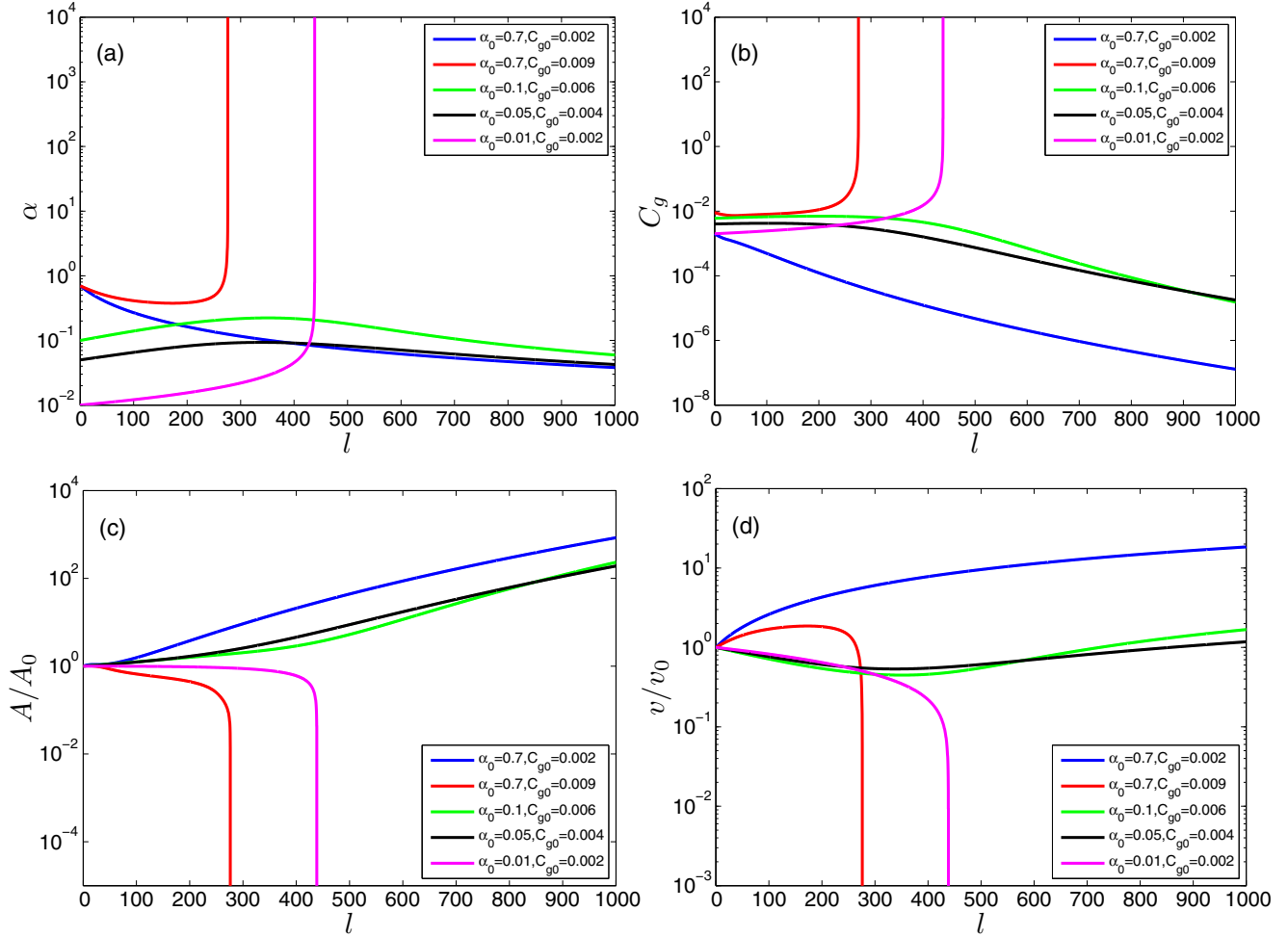By demanding these two equations to vanish, it is easy to find two infrared fixed points, namely a Gaussian fixed point

FIG. 6. Flows of parameters α, C_g, A, and v are shown in (a), (b), (c), and (d), respectively, in the presence of random chemical potential in the weak-coupling limit. Here, the fermion flavor is assumed to be $N = 2$.

$(\alpha_N^\star, C_g^\star) = (0,0)$ and a finite fixed point

$$(\alpha_N^\star, C_g^\star) = (1/\sqrt{e}, 1/4\pi^2 N \sqrt{e}). \tag{64}$$

The concrete flow diagram of α and C_g is plotted in Fig. 5(c), which shows that the finite fixed point is unstable. Upon leaving this point, α_N and C_g either flow to the Gaussian fixed point, or flow to larger values with growing l. Unfortunately, it is not clear how α_N and C_g evolute to the strong-coupling regimes due to our poor knowledge of the intermediate regime of Coulomb interaction. In the following, we concentrate on the low-energy properties of the system in the vicinity of the Gaussian fixed point. The flows of C_g, α_N, A, and v with varying l are depicted in Figs. 6(a)–6(d), respectively. It is interesting that v exhibits a nonmonotonic dependence on l for some specific initial values. When α_N and C_g flow to the Gaussian fixed point, $A(l)$ and $v(l)$ display nearly linear dependence on l for large l, which implies that $A(l)$ and $v(l)$ still receive weak logarithmic-like corrections before α_N and C_g flowing to zero.

3. Quasiparticle residue Z_f

After specifying the possible fixed points, we now examine whether the system exhibits non-FL behaviors. Now the

quasiparticle residue Z_f will be recalculated after taking into account the interplay of Coulomb interaction and random chemical potential. Using Eq. (48), we have

$$Z_f = e^{-\int_0^l (\gamma_z + C_g) dl}. \tag{65}$$

Although α_N and C_g flow to the trivial fixed point in the weak-coupling limit, $A(l)$ and $v(l)$ receive logarithmic corrections. The l dependence of Z_f is shown in Fig. 5(d), which manifests that $Z_f(l)$ decreases much more slowly than an exponential function. In particular, in the weak-coupling limit, random chemical potential can be nearly ignored and weak Coulomb interaction governs the low-energy behaviors of the system, which exhibits non- and marginal FL behaviors over a wide range of energy regimes [26].

B. Random mass

In this section, we consider the interplay of Coulomb interaction and random mass, and show that it results in quite different properties in the strong-coupling limit comparing to the case of random chemical potential. However, in the weak-coupling limit, the RG flow for the strength of random mass is similar, but not identical, to random chemical potential.
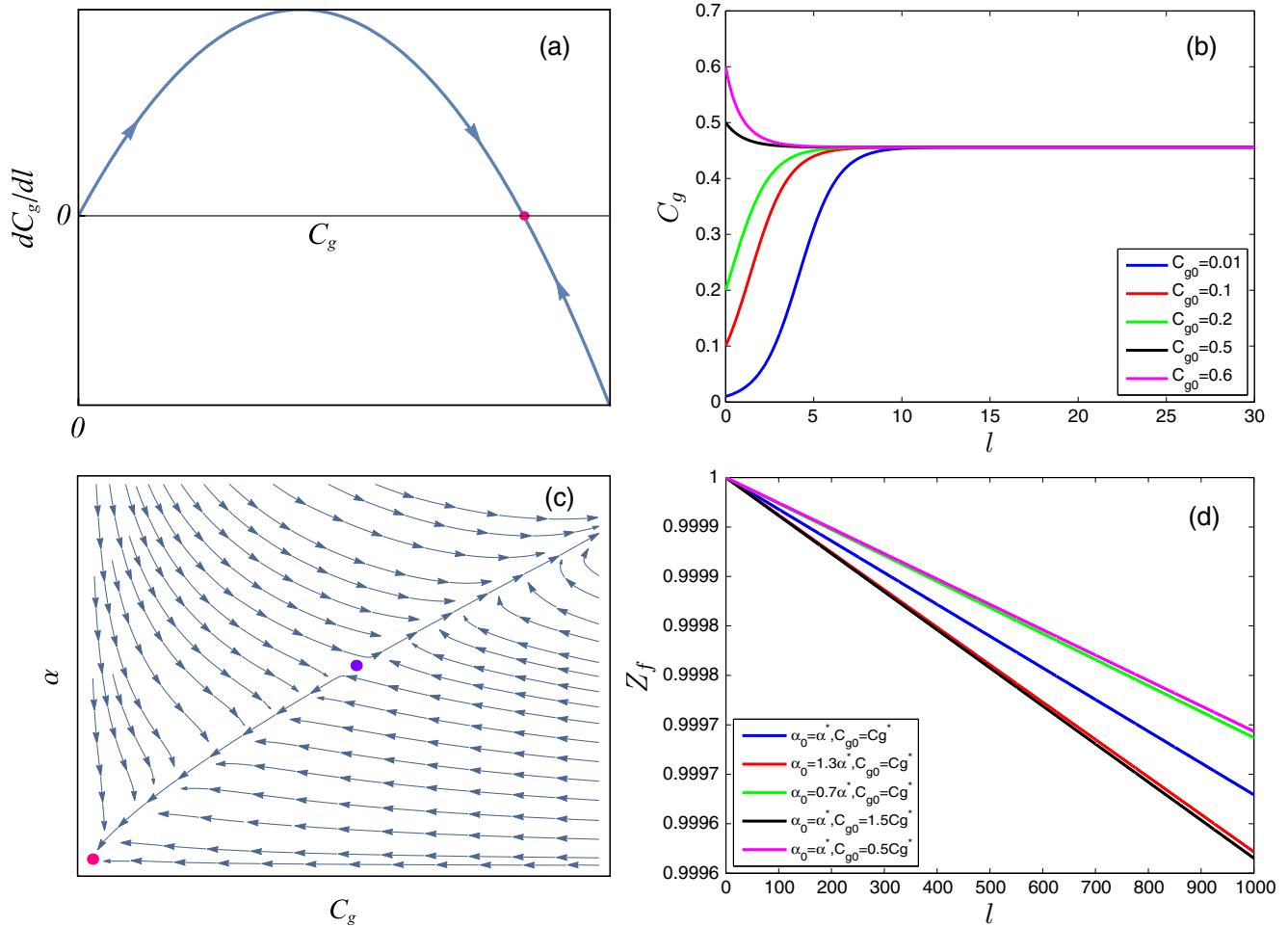
FIG. 7. (a) Flow diagram of C_g for random mass obtained in the strong-coupling limit. There is a table fixed point $C_g = a_m$. (b) Dependence of C_g on running length scale l for different initial values of C_{g0}. The existence of stable fixed point of C_g can be clearly seen. (c) Flow diagram in the space spanned by α and C_g for random mass, where α is in the weak coupling limit. The purple and red points represent two fixed points. (d) Flow of Z_f due to interplay of weak Coulomb interaction and random mass. Here, the fermion flavor is assumed to be $N = 2$.

1. Strong-coupling limit

In the strong-coupling regime with $\alpha_N \gg 1$, the RG equation of C_g is given by

$$\frac{dC_g}{dl} = (-2C_g + 2\gamma_D - \gamma_A - \gamma_v)C_g, \qquad (66)$$

where $\gamma_D = \frac{1.1564}{N}$. Its solution has the following form:

$$C_g(l) = \frac{a_m C_{g0} e^{2a_m l}}{C_{g0}(e^{2a_m l} - 1) + a_m}, \qquad (67)$$

where

$$a_m = \gamma_D - \frac{\gamma_A + \gamma_v}{2} = \frac{0.9121}{N}. \qquad (68)$$

The parameter C_g has two infrared fixed points: an unstable fixed point $C_g^\star = 0$, and a stable fixed point $C_g^\star = a_m$. The existence of these two fixed points can be clearly seen from Figs. 7(a) and 7(b). Recall that random mass is marginally irrelevant in the noninteracting limit. Our RG analysis show that the strong Coulomb interaction promotes random mass to become marginally relevant. In addition, it can be deduced from Eq. (36) that the Coulomb interaction parameter α

increases indefinitely as $l \to +\infty$. Comparing this result to the clean limit [26], we can see that the importance of Coulomb interaction is also significantly enhanced by random mass provided that the initial value of α_N is sufficiently large. Therefore the roles played by strong Coulomb interaction and random mass are both substantially promoted by their interplay.

To illustrate the mutual promotion, we now analyze the low-energy behaviors of parameters A and v, and discuss how they are influenced by the interplay of Coulomb interaction and random mass. Substituting Eq. (67) into Eqs. (32) and (33), then solving the differential equations, we obtain

$$F(l) = \frac{F_0 e^{\gamma_F l}}{\sqrt{t_m(e^{2a_m l} - 1) + 1}}, \qquad (69)$$

where $t_m \equiv C_{g0}/a_m$ and once again F stands for A or v. Since $0 < \gamma_F < a_m$, for very large l, $F(l)$ behaves asymptotically as

$$F(l)\big|_{l \to \infty} \sim F_0 e^{(\gamma_F - a_m)l}\big|_{l \to \infty} \to 0, \qquad (70)$$

which shows that $A(l)$ and $v(l)$ both vanish at large l.

Similar to the case of random chemical potential, the parameter α_N also flows to very large values without upper
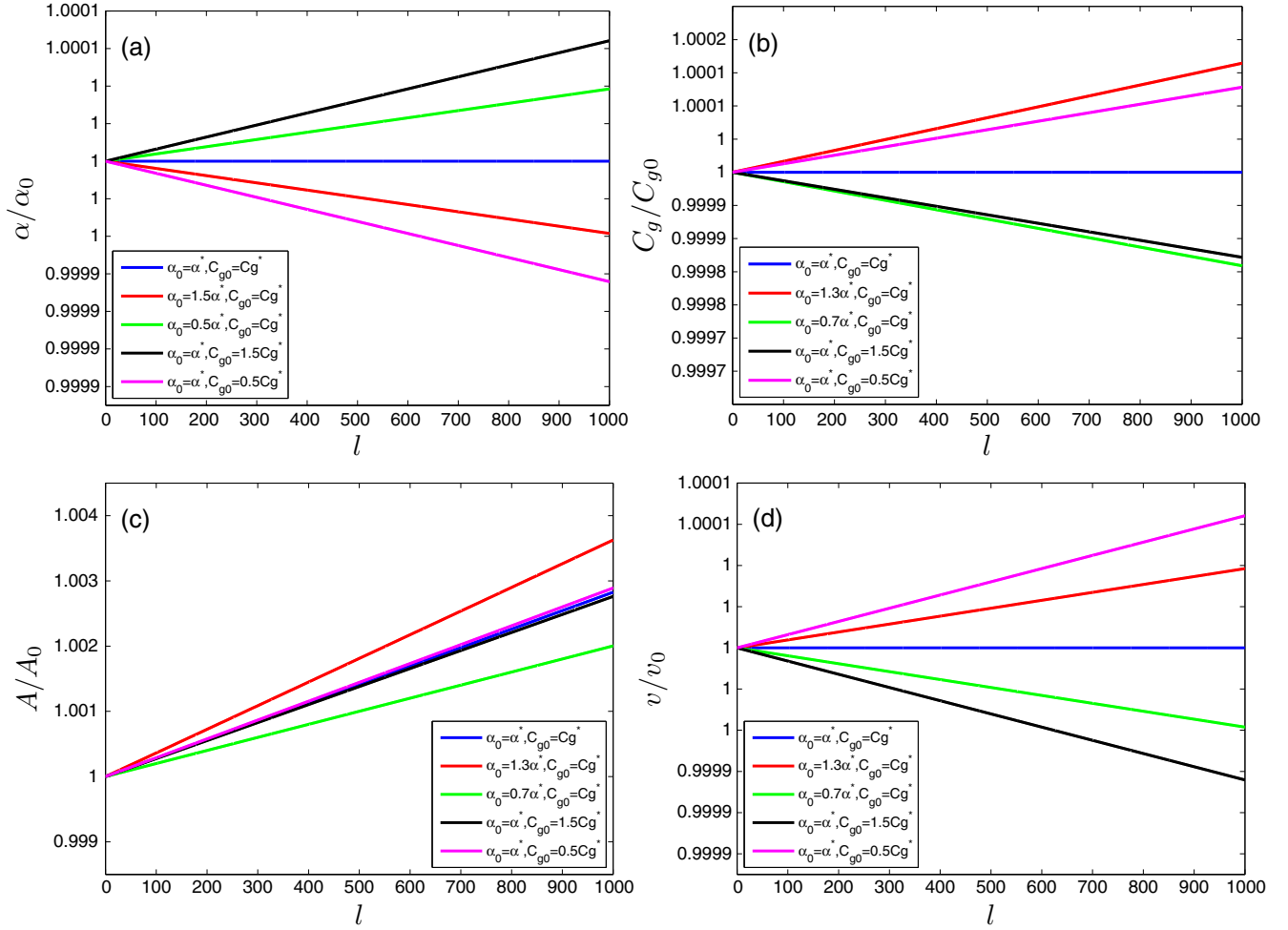
FIG. 8. Flows of α, C_g, A, and v due to interplay of Coulomb interaction and random mass are shown in (a), (b), (c), and (d), respectively. The results are obtained in the weak-coupling limit of α. $\alpha^\star$ and $C_g^\star$ stand for the values of α and C_g at the unstable fixed point, respectively. Here, the fermion flavor is assumed to be $N = 2$.

bound, but the parameter C_g for random mass flows to certain finite value. Based on Eq. (65), Z_f can be written as

$$Z_f(l)\big|_{l\to+\infty} = e^{-\delta l}, \tag{71}$$

where $\delta > a_m$ for large α_N. Making the same analysis as presented in Sec. IV B, we find that the interplay of strong Coulomb interaction and random mass drives the system to become a non-FL, even in the lowest energy limit.

2. Weak-coupling limit

We now study the interplay of Coulomb interaction and random mass supposing the initial value of strength of Coulomb interaction is small. Following the computational steps presented in Sec. V A 2, we have solved the corresponding RG equations. According to the flow diagram depicted in Fig. 7(c), there are a stable fixed point $(\alpha_N^\star, C_g^\star) = (0,0)$ and an unstable fixed point

$$(\alpha_N^\star, C_g^\star) = \left(e^{-\frac{23}{2}}, e^{-\frac{23}{2}}/4\pi^2 N\right). \tag{72}$$

The detailed l-dependence of the parameters α_N, C_g, A, and v are presented in Figs. 8(a)–8(d), respectively. From Figs. 8(a)

and 8(b), we observe that α and C_g flow to distinct regimes when their initial values take different values. Moreover, Figs. 8(c) and 8(d) show that, $A(l)$ always increases over a broad range of l, but $v(l)$ may either increase or decrease, depending on the initial values of α_N and C_g.

From the above analysis made in the strong and weak-coupling regimes of Coulomb interaction, we conclude that the low-energy behaviors of 2D SDFs are mainly determined by the initial value of interaction parameter α_N. The SDF system exhibits distinct properties at large and small values of α_N. The quasiparticle residue Z_f due to strong Coulomb interaction and random mass is already given in Eq. (71). In the weak-coupling limit, both α_N and C_g flow to zero. In this case, $Z_f(l)$ cannot be expressed in such a power-law function as Eq. (71). We plot the variation of Z_f with l in Fig. 7(d), which exhibits that $Z_f(l)$ decreases much more slowly than an exponential function. Thus, in the weak-coupling limit, random mass does not induce remarkably qualitative change for the behavior of Z_f if the system is driven to the Gaussian fixed point $(\alpha_N^\star, C_g^\star) = (0,0)$. As α_N decreases from certain large value down to some small value, the SDF system is altered from a non-FL to a marginal FL. However, since the intermediate coupling regime is technically hard to access,
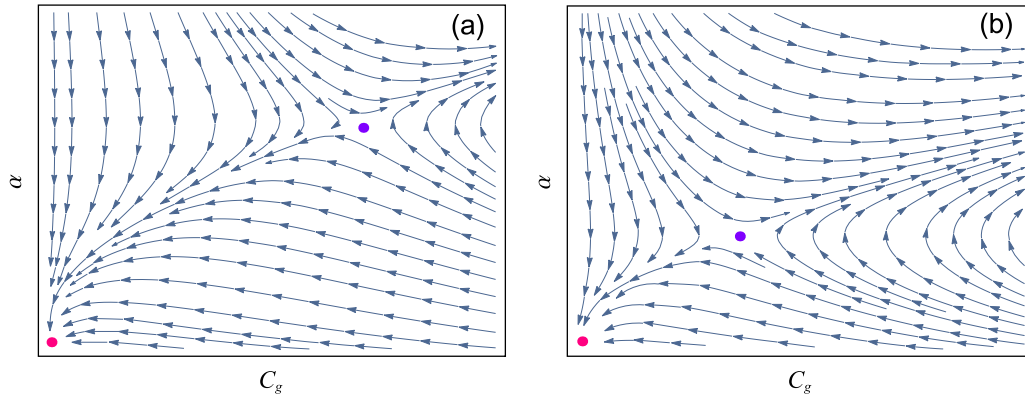
FIG. 9. Flow diagram in the space spanned by α and C_g for τ_x component of random gauge potential is shown in (a) and τ_y component in (b), where α in the weak-coupling limit. The red and purple points represent the Gaussian fixed point and unstable finite fixed point, respectively. Here, the fermion flavor is assumed to be $N = 2$.

it remains unclear whether this is a phase transition or a crossover, and further research is required to address this issue.

C. Random gauge potential

In the case of random gauge potential, the flow equation for C_g is

$$\frac{dC_g}{dl} = (2\gamma_D - \gamma_A - \gamma_v)C_g \qquad (73)$$

in the strong-coupling limit. Here, γ_D take different values for the τ_x and τ_y components. However, since $\gamma_D > (\gamma_A + \gamma_v)/2$ for both components, it is clear that $C_g(l)$ increases monotonously as l grows, and tends to diverge in the limit $l \rightarrow +\infty$. Therefore, although random gauge potential is marginal in the noninteracting limit, it becomes relevant due to strong Coulomb interaction. Moreover, the parameters A and v are driven to vanish at the lowest energy. From Eq. (36), we see that α_N also increases indefinitely as $l \longrightarrow +\infty$. Thus the effective strength of Coulomb interaction is remarkably enhanced by random gauge potential, and indeed becomes a relevant perturbation. As already explained in the above discussions, one reasonable interpretation of the indefinite increase of α_N and C_g with growing l is that the system becomes insulating.

We finally consider the weak-coupling limit. For the τ_x-component of random gauge potential, the flow diagram is depicted in Fig. 9(a), and that of τ_y-component in Fig. 9(b). Both of these two flow diagrams contain a stable Gaussian fixed point and an unstable finite fixed point. The RG flows of α_N and C_g are analogous to those obtained in the cases of random chemical potential and random, which has been discussed in great detail in the last two sections.

performing extensive RG calculations, we have showed that Coulomb interaction and disorder can substantially affect each other, which then leads to a series of interesting phases and transitions between distinct phases. The concrete results obtained in the presence of three types of disorders have already been summarized at the end of Sec. I, and thus are not repeated here.

Due to technical difficulties, we are not able to handle the case in which the Coulomb interaction strength α_N is neither small nor large. The results obtained in this work are applicable only to the weak and strong-coupling limits of Coulomb interaction.

The RG analysis have showed that the parameter α_N for Coulomb interaction can flow to very large values due to its interplay with disorders. A reasonable explanation for this behavior is that a certain quantum phase transition happens, which induces an instability of the system and prevents α_N from really flowing to infinity. However, the nature of such a phase transition is still not clear. Generically, the 2D SDSM may become an excitonic insulator [10,73–82], or even a Wigner lattice [72]. Further studies are certainly needed to identify the true ground state of such an extremely correlated fermion system. To examine whether it is possible to form an excitonic insulator, one should go beyond the perturbative expansion method, and study the excitonic insulating transition by using the self-consistent Dyson-Schwinger equation approach [10,73–76,79–82]. When the Coulomb interaction is sufficiently strong, the fermions may acquire a dynamically generated mass term, $\propto m\tau_z$, which then drives the system to enter into an excitonic insulating phase [10,73–82]. This work is now in progress, and will be presented in a separate paper [83]. Large-scale numerical simulations are also expected to provide useful information [77,78].

VI. SUMMARY AND DISCUSSION

We have studied the quantum phase transitions and non-FL behaviors induced by the interplay of Coulomb interaction and disorder in a 2D SDSM in which the fermion dispersion is linear in one direction and quadratic in the other. After

[1] A. A. Abrikosov, L. P. Gorkov, and I. E. Dyaloshinski, *Methods of Quantum Field Theory in Statistical Physics* (Dover, New York, 1975).

[2] G. F. Giuliani and G. Vignale, *Quantum Theory of the Electron Liquid* (Cambridge University Press, Cambridge, 2005)

[3] B. L. Altshuler and A. G. Aronov, in *Electron-Electron Interaction in Disordered Systems*, edited by M. Pollak and A. L. Efros (North-Holland, Amsterdam, 1984).

[4] P. A. Lee and T. V. Ramakrishnan, Rev. Mod. Phys. **57**, 287 (1985).

[5] D. Belitz and T. R. Kirkpatrick, Rev. Mod. Phys. **66**, 261 (1994).

[6] E. Abrahams, S. V. Kravchenko, and M. R. Sarachik, Rev. Mod. Phys. **73**, 251 (2001).

[7] A. Altland, B. D. Simons, and M. R. Zirnbauer, Phys. Rep. **359**, 283 (2002).

[8] A. H. Castro Neto, F. Guinea, N. M. R. Peres, K. S. Nonoselov, and A. K. Geim, Rev. Mod. Phys. **81**, 109 (2009).

[9] S. D. Sarma, S. Adam, E. H. Hwang, and E. Rossi, Rev. Mod. Phys. **83**, 407 (2011).

[10] V. N. Kotov, B. Uchoa, V. M. Pereira, F. Guinea, and A. H. Casto Neto, Rev. Mod. Phys. **84**, 1067 (2012).

[11] O. Vafek and A. Vishwanath, Annu. Rev. Condens. Matter Phys. **5**, 83 (2014).

[12] T. O. Wehling, A. M. Black-Schaffer, and A. V. Balatsky, Adv. Phys. **63**, 1 (2014).

[13] J. Gonzalez, F. Guinea, and M. A. H. Vozmediano, Phys. Rev. B **59**, R2474(R) (1999).

[14] J. Hofmann, E. Barnes, and S. Das Sarma, Phys. Rev. Lett. **113**, 105502 (2014).

[15] P. Goswami and S. Chakravarty, Phys. Rev. Lett. **107**, 196803 (2011).

[16] P. Hosur, S. A. Parameswaran, and A. Vishwanath, Phys. Rev. Lett. **108**, 046602 (2012).

[17] R. E. Throckmorton, J. Hofmann, E. Barnes, and S. Das Sarma, Phys. Rev. B **92**, 115101 (2015).

[18] E. G. Moon, C. Xu, Y. B. Kim, and L. Balents, Phys. Rev. Lett. **111**, 206401 (2013).

[19] A. A. Abrikosov and S. D. Baneslavskii, Sov. Phys. JETP **32**, 699 (1971).

[20] A. A. Abrikosov, Sov. Phys. JETP **39**, 709 (1974).

[21] B.-J. Yang, E.-G. Moon, H. Isobe, and N. Nagaosa, Nat. Phys. **10**, 774 (2014).

[22] A. A. Abrikosov, J. Low Tem. Phys. **8**, 315 (1972).

[23] H.-H. Lai, Phys. Rev. B **91**, 235131 (2015).

[24] S.-K. Jian and H. Yao, Phys. Rev. B **92**, 045121 (2015).

[25] Y. Huh, E.-G. Moon, and Y. B. Kim, Phys. Rev. B **93**, 035138 (2016).

[26] H. Isobe, B.-J. Yang, A. Chubukov, J. Schmalian, and N. Nagaosa, Phys. Rev. Lett. **116**, 076803 (2016).

[27] G. Y. Cho and E.-G. Moon, Sci. Rep. **6**, 19198 (2016).

[28] L.-K. Lim, J.-N. Fuchs, and G. Montambaux, Phys. Rev. Lett. **108**, 175303 (2012).

[29] B. Dóra, I. F. Herbut, and R. Moessner, Phys. Rev. B **88**, 075126 (2013).

[30] P. Delplace, Á. Gomez-Léon, and G. Platero, Phys. Rev. B **88**, 245422 (2013).

[31] H.-Q. Huang, Z.-R. Liu, H.-B. Zhang, W.-H. Duan, and D. Vanderbilt, Phys. Rev. B **92**, 161115(R) (2015).

[32] P. K. Pyatkovskiy and T. Chakraborty, Phys. Rev. B **93**, 085145 (2016).

[33] G. Montambaux, F. Piechon, J.-N. Fuchs, and M. O. Goerbig, Eur. Phys. J. B **72**, 509 (2009).

[34] G. Montambaux, F. Piechon, J.-N. Fuchs, and M. O. Goerbig, Phys. Rev. B **80**, 153412 (2009).

[35] P. Dietl, F. Pichon, and G. Montambaux, Phys. Rev. Lett. **100**, 236405 (2008).

[36] S. Katayama, A. Kobayashi, and Y. Suzumura, J. Phys. Soc. Jpn. **75**, 054705 (2006).

[37] A. Kobayashi, S. Katayama, Y. Suzumura, and H. Fukuyama, J. Phys. Soc. Jpn. **76**, 034711 (2007).

[38] M. O. Goerbig, J.-N. Fuchs, G. Montambaux, and F. Piéchon, Phys. Rev. B **78**, 045415 (2008).

[39] V. Pardo and W. E. Pickett, Phys. Rev. Lett. **102**, 166803 (2009).

[40] V. Pardo and W. E. Pickett, Phys. Rev. B **81**, 035111 (2010).

[41] S. Banerjee, R. R. P. Singh, V. Pardo, and W. E. Pickett, Phys. Rev. Lett. **103**, 016402 (2009).

[42] P. Delplace and G. Montambaux, Phys. Rev. B **82**, 035438 (2010).

[43] S. Banerjee and W. E. Pickett, Phys. Rev. B **86**, 075124 (2012).

[44] M. Ezawa, New J. Phys. **16**, 115004 (2014).

[45] Q. Liu, X. Zhang, L. B. Abdalla, A. Fazzio, and A. Zunger, Nano Lett. **15**, 1222 (2015).

[46] K. Dolui and S. Y. Quek, Sci. Rep. **5**, 11699 (2015).

[47] Z. J. Xiang, G. J. Ye, C. Shang, B. Lei, N. Z. Wang, K. S. Yang, D. Y. Liu, F. B. Meng, X. G. Luo, L. J. Zou, Z. Sun, Y. B. Zhang, and X. H. Chen, Phys. Rev. Lett. **115**, 186403 (2015).

[48] P.-L. Gong, D.-Y. Liu, K.-S. Yang, Z.-J. Xiang, X.-H. Chen, Z. Zeng, S.-Q. Shen, and L.-J. Zou, Phys. Rev. B **93**, 195434 (2016).

[49] J. Kim, S. S. Baik, S. H. Ryu, Y. Sohn, S. Park, B.-G. Park, J. Denlinger, Y. Yi, H. J. Choi, and K. S. Kim, Science **349**, 723 (2015).

[50] E. Abrahams, P. W. Anderson, D. C. Licciardello, and T. V. Ramakrishnan, Phys. Rev. Lett. **42**, 673 (1979).

[51] A. W. W. Ludwig, M. P. A. Fisher, R. Shankar, and G. Grinstein, Phys. Rev. B **50**, 7526 (1994).

[52] T. Stauber, F. Guinea, and M. A. H. Vozmediano, Phys. Rev. B **71**, 041406(R) (2005).

[53] I. F. Herbut, V. Juričić, and O. Vafek, Phys. Rev. Lett. **100**, 046403 (2008).

[54] O. Vafek and M. J. Case, Phys. Rev. B **77**, 033410 (2008).

[55] J.-R. Wang and G.-Z. Liu, Phys. Rev. B **89**, 195404 (2014).

[56] E.-G. Moon and Y. B. Kim, arXiv:1409.0573.

[57] D. Carpentier, A. A. Fedorenko, and E. Orignac, Europhys. Lett. **102**, 67010 (2013).

[58] A. M. Finkelstein, Z. Phys. B: Condens. Matter **56**, 189 (1984).

[59] A. Punnoose and A. M. Finkelstein, Science **310**, 289 (2005).

[60] A. A. Nersesyan, A. M. Tsvelik, and F. Wenger, Nucl. Phys. B **438**, 561 (1995).

[61] J. Wang, G.-Z. Liu, and H. Kleinert, Phys. Rev. B **83**, 214503 (2011).

[62] R. Shankar, Rev. Mod. Phys. **66**, 129 (1994).

[63] B. Roy and S. Das Sarma, Phys. Rev. B **90**, 241112(R) (2014).

[64] E. Fradkin, Phys. Rev. B **33**, 3257 (1986); **33**, 3263 (1986).

[65] R. Shindou and S. Murakami, Phys. Rev. B **79**, 045321 (2009).

[66] S. V. Syzranov, L. Radzihovsky, and V. Gurarie, Phys. Rev. Lett. **114**, 166601 (2015).

[67] K. Kobayashi, T. Ohtsuki, K. I. Imura, and I. F. Herbut, Phys. Rev. Lett. **112**, 016402 (2014).

[68] R. R. Biswas and S. Ryu, Phys. Rev. B **89**, 014205 (2014).

[69] J.-R. Wang, G.-Z. Liu, and C.-J. Zhang, New J. Phys. **18**, 073023 (2016).

[70] Z. Yang, C. Ko, V. Balakrishnan, G. Gopalakrishnan, and S. Ramanathan, Phys. Rev. B **82**, 205101 (2010).

[71] T. Nagahama, M. Kobayashi, Y. Akahama, S. Endo, and S.-i. Narita, J. Phys. Soc. Jpn. **54**, 2096 (1985).

[72] B. Tanatar and D. M. Ceperley, Phys. Rev. B **39**, 5005 (1989).

[73] D. V. Khveshchenko, Phys. Rev. Lett. **87**, 246802 (2001).

[74] E. V. Gorbar, V. P. Gusynin, V. A. Miransky, and I. A. Shovkovy, Phys. Rev. B **66**, 045108 (2002).

[75] D. V. Khveshchenko and H. Leal, Nucl. Phys. B **687**, 323 (2004).

[76] G.-Z. Liu, W. Li, and G. Cheng, Phys. Rev. B **79**, 205429 (2009).

[77] S. Hands and C. Strouthos, Phys. Rev. B **78**, 165423 (2008).

[78] J. E. Drut and T. A. Lahde, Phys. Rev. Lett. **102**, 026802 (2009).

[79] D. V. Khveshchenko, J. Phys: Condens. Matter **21**, 075303 (2009).

[80] O. V. Gamayun, E. V. Gorbar, and V. P. Gusynin, Phys. Rev. B **81**, 075429 (2010).

[81] J.-R. Wang and G.-Z. Liu, New J. Phys. **14**, 043036 (2012).

[82] C. Popovici, C. S. Fischer, and L. von Smekal, Phys. Rev. B **88**, 205429 (2013).

[83] J.-R. Wang, G.-Z. Liu, and C.-J. Zhang (unpublished).